Hybrid mode matching method for the efficient analysis of metal and dielectric rods in H plane rectangular waveguide devices

Carmen Bachiller*, Héctor Esteban*, Hilario Mata*, María Ángeles Valdés*, Vicente Enrique Boria*, Ángel Belenguer†, José Vicente Morro*

* Universidad Politécnica de Valencia, Spain
e-mail: mabacmar@dcom.upv.es

† Universidad de Castilla La Mancha, Spain
email: angel.belenguer@uclm.es

***Abstract*— The paper presents a new accurate and efficient technique for the analysis of H-plane single or multiple rods in rectangular waveguides. The new method is based on a mode matching procedure that matches open space and guided modes along a circular boundary that encloses the rods. Since the EM fields around the obstacles are expanded using open space cylindrical modes, a full analytical (and highly efficient) solution can be obtained for dielectric or metallic circular posts. However, this technique can also cope with any arbitrary geometry of the H plane obstacles. In such a case, a numerical method should be used to characterize geometries other than circular in terms of cylindrical modes, and therefore the efficiency would be reduced.**

The method has been successfully applied to the analysis and design of several H plane filters with different topologies involving single centered and off-centered posts, as well as double post geometries.

***Index Terms*— Microwave filters, Rectangular waveguides, Mode matching methods, Dielectric loaded waveguides.**

I. Introduction

Circular metallic and dielectric rods inside a rectangular waveguide are frequently found in the geometry of many passive microwave devices, such as passband or stopband filters, diplexers or oscillators [1], [2]. Ceramic dielectrics with high dielectric constant and temperature stability are commercially available. They allow the replacement of bulky and expensive waveguide resonant cavities in microwave filters or oscillators by low-cost, small size, good temperature stability, and high-Q dielectric resonators [3], [4]. If the height of the dielectric posts is the same as the height of the waveguide, that is, if the posts are all inductive or H-plane, better out of band rejection and multipactor response can be obtained [5].

The authors have developed a technique for the analysis of these passive devices which consists on dividing the device in simpler building blocks: empty waveguides, steps and sections of waveguide loaded with the dielectric or metallic posts. The generalized scattering matrix of each block is obtained by the most suitable analysis method, and then all the matrices are connected by a new and efficient iterative technique [6] that provides the generalized scattering matrix of the whole filter.

For instance, the generalized scattering matrix of the empty sections of the waveguide is well known from the literature [7], and the waveguide step can be analyzed by means of several modal techniques, such as the well know mode matching method [8] or the integral equation technique [9].

However, the analysis of waveguide sections loaded with circular obstacles is far more complex. In order to characterize these structures, circular and rectangular geometries must be considered at the same time. This complexity in the geometry makes it difficult to use purely analytic techniques,while the numerical methods are highly time-consuming. This is a serious drawback when using the simulator in a design process, since it typically demands a huge number of simulations before it finds a suitable design that fulfils the specifications. For this reason the accurate and efficient analysis of H-plane circular rods inside rectangular waveguides has received considerable attention for more than 60 years.

Using variational methods, Marcuvitz [10] calculated the circuit parameters of circular posts of small radius. This method was invalid near resonance. Lewin [11] calculated the reflection coefficient of a metallic post assuming that the radius was small. Araneta *et al.* [12] improved the variational method attributed to Schwinger and used by Marcuvitz in [10], and was able to accurately analyze large dielectric circular rods.

Leviatan *et al.* [13] developed a moment solution for the analysis of a single circular metallic post placing fictitious currents inside the post. Next a multiple point matching of the boundary condition is applied and the unknown filamentary currents are obtained. This allows the accurate analysis of large posts. This method was extended in [14], [15] and [16] to, respectively, the analysis of multiple metallic posts, multiple dielectric posts and multilayer posts of arbitrary and smooth cross section.

Hsu and Auda [3] derived a volume integral field equation for the equivalent polarization current of a general problem of multiple dielectric posts of arbitrary cross section. This equation was solved numerically using a subsectional point matching moment method.

Koshiba and Suzuki [17] applied a combination of the finite

element method and an analytical method to the analysis of H-plane waveguide junctions with an arbitrarily shaped ferrite post, such as the Y-junction circulator with ferrite post. Ise and Koshiba [18], [19] used a combination of the finite and boundary element methods to solve the scattering of circular dielectric posts. Then, they derive the corresponding equivalent circuit using a lattice network and demonstrated the three different types of resonances of the dielectric post inside a waveguide. Similarly, Auda and Smith [20] applied the resonance method for evaluating the impedances of the equivalent network of a dielectric post.

In [4], Arcioni *et al.* use the boundary integral-resonant mode expansion (BI-RME) method to the analysis of H-plane cavities with dielectric resonators, where both the cavity and the dielectric post can be of arbitrary cross section. Catina *et al.* [21] use a surface integral method for the analysis of any arbitrarily shaped 2D problem including dielectric posts.

Recently, Bhattacharya and Gupta [22] have used a neural network model for the analysis of a circular dielectric post.

Nielsen [23] was the first to characterize a circular post using open space cylindrical waves. Then a discrete mode-matching with the external guided waves of the rectangular waveguide was performed using a rectangular boundary which included the waveguide walls in order to calculate the circuit parameters. In [24] Lewin discussed the inadequacy of the discrete mode-matching technique with some waveguide discontinuities problems, such as the geometry used by Nielsen. To overcome this limitation, Sahalos and Vafiadis [25] used a circular boundary to perform the discrete mode-matching between cylindrical and guided waves, thus avoiding the waveguide walls in the boundary region. This improves the convergence rate, although only centered circular posts can still be analyzed. Geshe and Löchel [26] also used a cylindrical boundary and cylindrical waves inside and guided waves outside that boundary to expand the fields. Using the orthogonal expansion method, they forced field continuity at the cylindrical boundary and obtained the scattering parameters of an off-centered dielectric cylinder with not too large radius and permittivity values. This method provides the field distribution and Poynting vector inside the waveguide and the cylinder. The same authors extended their method to the analysis of resonators with two cylinders in [27]. Abdulnour and Marchildon [28] analyzed circular and rectangular posts using, respectively, rectangular and circular boundaries. Instead of using point matching as previous authors did, they used an integral method which converges faster and provides more accurate results, but they must perform numerical integration.

In [29] Esteban *et al.* also used a circular boundary to match cylindrical and guided waves, so that they could analyze an arbitrarily shaped H-plane post, providing greater accuracy and efficiency than previous methods, and being able to analyze any arbitrary geometry. However, when this method is used to compute the generalized scattering matrix of a large post placed very close to other discontinuities (i.e. steps), which is the case of some filtering structures, an instability in the results appears. This is because in those cases the accuracy of the results is limited to the fundamental mode, since there is a poor accuracy for the coefficients of the scattering matrix correspondant to higher order modes. This means that when the scattering matrix of the post is cascaded with the matrices of adjacent building blocks of the structure (i.e. steps, lines), the overall accuracy rapidly decreases and the whole filter response is not correct.

In this paper the authors propose an improvement of the method presented in [29] in order to increase the accuracy and stability of the analysis, no matter the number of modes or the nature of the H-plane problem under study. This is accomplished with a new mode matching procedure which uses the fast Fourier transform to solve the matching between cylindrical and guided modes. Analytical expressions are used to characterize the circular posts in the inner region, thus resulting in a highly efficient technique for the analysis of single or multiple posts inside a rectangular waveguide.

II. Description of the Method

In order to characterize one or various metallic or dielectric rods placed inside a rectangular waveguide, two regions are defined (see Fig. 1).

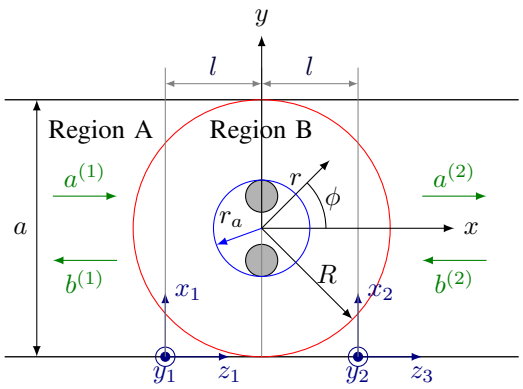

Fig. 1. General layout of the problem and different regions for the analysis method

In order to find the circuit parameters of the structure, the fields in region B are expanded in series of cylindrical modes and the fields in region A in series of guided modes. Next a mode matching is performed between the guided modes of region A and the cylindrical modes of region B, enforcing the continuity of the tangential electric and magnetic fields across the circular boundary and projecting the resulting equations to the modes of regions A and B.

In region B the field is expanded as summations of incident and scattered cylindrical open space modes,

$$\vec{E} = \vec{E}^{in}(\rho,\phi) + \vec{E}^{sc}(\rho,\phi) \quad (1)$$

$$\vec{E}^{in}(\rho,\phi) = \sum_{n=-N_i}^{N_i} i_n J_n(k\rho) e^{jn\phi}\hat{z} \quad (2)$$

$$\vec{E}^{sc}(\rho,\phi) = \sum_{q=-N_{sc}}^{N_{sc}} c_q H_q^{(2)}(k\rho) e^{jq\phi}\hat{z} \quad (3)$$

where i_n and c_q are the incident and scattered field spectra in open space, $J_n(k\rho(\phi))e^{jn\phi}$ and $H_q^{(2)}(k\rho(\phi))e^{jq\phi}$ are the n-th incident and q-th scattered cylindrical modes, and N_i and

N_{sc} are the truncation indexes for the summations of incident and scattered cylindrical modes. Both numbers must be high enough to ensure good accuracy of the results [29].

In region B, the scattered field spectrum c_q can be related to the incident field spectrum i_n by means of a scattering matrix D that provides the full wave characterization of the scattering structure inside region B [29], and so we can write

$$c_q = \sum_{q=-N_i}^{N_i} d_{qn}\, i_n \tag{4}$$

In matrix form $c = D\, i$. Using (4), the scattered field is

$$\overrightarrow{E}^{sc}(\rho,\phi) = \sum_{q=-N_{sc}}^{N_{sc}} \sum_{n=-N_i}^{N_i} d_{qn}\, i_n H_q^{(2)}(k\rho) e^{jq\phi}\hat{z} \tag{5}$$

In the outer region, or region A, the tangential fields are expanded as summations of the guided modes of the canonical rectangular waveguide. Since both the geometry and the excitation are invariant in height (dimension z), only the family of TE_{m0} modes are considered, and the fields can be expanded as

$$\vec{E}_t^{(i)} = \sum_{m=1}^{Mi} (a_m^{(i)} e^{-\gamma_m^{(i)} z_i} + b_m^{(i)} e^{\gamma_m^{(i)} z_i}) \vec{e}_m^{(i)'}(x_i) \tag{6}$$

$$\vec{H}_t^{(i)} = \sum_{m=1}^{Mi} (a_m^{(i)} e^{-\gamma_m^{(i)} z_i} - b_m^{(i)} e^{\gamma_m^{(i)} z_i}) Y_{0m}^{(i)} \vec{h}_m^{(i)'}(x_i) \tag{7}$$

where $i = 1$ for the input port and $i = 2$ for the output port, and

$$\vec{e}_m^{(i)'}(x_i) = \hat{y}_i \sqrt{\frac{2Z_{0m}^{(i)}}{a_i b_i}} \sin\left(\frac{m\pi}{a_i} x_i\right) \tag{8}$$

$$\vec{h}_m^{(i)'}(x_i) = -\hat{x}_i \sqrt{\frac{2Z_{0m}^{(i)}}{a_i b_i}} \sin\left(\frac{m\pi}{a_i} x_i\right) \tag{9}$$

$$\gamma_m^{(i)} = \sqrt{\left(\frac{m\pi}{a_i}\right)^2 - k^2} \tag{10}$$

$$Y_{0m}^{(i)} = \frac{1}{Z_{0m}^{(i)}} = \frac{\gamma_m^{(i)}}{jw\mu} = \frac{\gamma_m^{(i)}}{jk\eta} \tag{11}$$

In these equations

- m is the index of the correspondant guided mode.
- M_i, a_i and b_i are, respectively, the number of guided modes, the width and the height of the input ($i = 1$) and output ($i = 2$) ports. In the structures considered in this work $M_2 = M_1$, $a_2 = a_1$ and $b_2 = b_1$.
- $a_m^{(i)}$ and $b_m^{(i)}$ are, respectively, the amplitudes of the waves in the input ($i = 1$) and output ($i = 2$) ports.
- x_i and z_i are the coordinates local to the input ($i = 1$) and output ($i = 2$) waveguides (see Fig. 1).

The amplitudes and admitances of the guided waves can be referenced in a more compact way defining the following vectors $\boldsymbol{a}$, $\boldsymbol{b}$ and $\boldsymbol{Y_0}$, each of one of $M = M_1 + M_2$ elements,

$$\boldsymbol{a} = \begin{bmatrix} a^{(1)} \\ b^{(2)} \end{bmatrix}, \boldsymbol{b} = \begin{bmatrix} b^{(1)} \\ a^{(2)} \end{bmatrix}, \boldsymbol{Y_0} = \begin{bmatrix} -Y_0^{(1)} \\ Y_0^{(2)} \end{bmatrix} \tag{12}$$

where

$$a^{(i)} = [a_1^{(i)}, \cdots, a_{M_i}^{(i)}]^T,\ i \in [1,2] \tag{13}$$

$$b^{(i)} = [b_1^{(i)}, \cdots, b_{M_i}^{(i)}]^T,\ i \in [1,2] \tag{14}$$

$$Y_0^{(i)} = [Y_{01}^{(i)}, \cdots, Y_{0M_i}^{(i)}]^T,\ i \in [1,2] \tag{15}$$

Using (12) we can express in a compact way the tangential fields outside the boundary,

$$\vec{E}_t(\phi) = \sum_{n=1}^{M} (a_n e_n^+(\phi) + b_n e_n^-(\phi)) g_n(\phi)\hat{z} \tag{16}$$

$$\vec{H}_t(\phi) = \sum_{n=1}^{M} (a_n e_n^+(\phi) - b_n e_n^-(\phi)) Y_{0n} g_n(\phi)\hat{y} \tag{17}$$

where $M = M_1 + M_2$ and,

$$e_n^{\pm}(\phi) = \begin{cases} e^{\mp\gamma_n^{(1)} z_1(\phi)} & \phi \in \left[\frac{\pi}{2}, \frac{3\pi}{2}\right],\ n \le M_1 \\ e^{\pm\gamma_{n-M_1}^{(2)} z_2(\phi)} & \phi \in \left[-\frac{\pi}{2}, \frac{\pi}{2}\right],\ n > M_1 \\ 0 & \text{other} \end{cases} \tag{18}$$

$$g_n(\phi) = \begin{cases} e_n^{(1)'}(x_1(\phi)) & \phi \in \left[\frac{\pi}{2}, \frac{3\pi}{2}\right],\ n \le M_1 \\ e_{n-M_1}^{(2)'}(x_2(\phi)) & \phi \in \left[-\frac{\pi}{2}, \frac{\pi}{2}\right],\ n > M_1 \\ 0 & \text{other} \end{cases} \tag{19}$$

The choice of a circular boundary for the mode matching avoids the waveguide walls in the boundary region. And instead of using discrete mode matching, in this work the mode matching is solved by projecting the equations resulting from enforcing field continuity to the modes of regions A and B. This provides with a set of equations, and after selecting the proper ones, a matrix system is obtained whose solution is the generalized scattering matrix of the structure. If the right set of equations is selected the matrix system is very well conditioned and a very good accuracy can be obtained. Moreover the integrals that must be solved in order to compute the elements of the matrices involved can be solved by using the fast Fourier transform instead of using other numerical methods.

The application of this mode matching procedure can be very simple if the obstacle is a centered circular post, but can be generalized for arbitrary single or multiple obstacles. In the next sections, we describe the mode matching procedure for the case of a single centered circular cylinder and for arbitrary obstacles. The theory of arbitrary obstacles has also been detailed for the cases of an off-centered circular post and for two circular posts.

III. Centered Circular Post

A. Generalized Scattering Matrix

When the post inside the circular boundary is a single centered circular post, as shown in Fig. 2, each incident cylindrical mode excites only the scattered cylindrical mode of the same order. Thus the scattering matrix that relates incident and scattered cylindrical spectra is a diagonal matrix, and

$$d_{qn} = 0, \quad \forall q \neq n \tag{20}$$

$$c_q = \sum_{n=-N_i}^{N_i} d_{qn}\, i_n = d_{qq}\, i_q \tag{21}$$

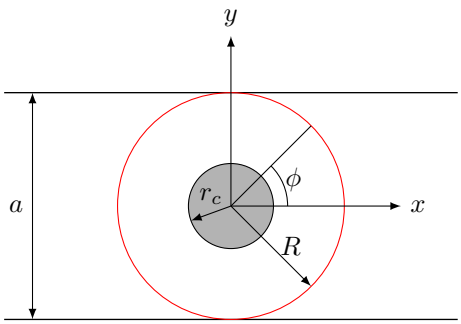

Fig. 2. Single centered circular cylinder.

And for a single centered circular cylinder the elements d_{nn} of the scattering matrix can be easily obtained analytically [30], either for a metallic

$$d_{nn} = -\frac{J_n(kr_c)}{H_n^{(2)}(kr_c)} \tag{22}$$

or a dielectric cylinder

$$d_{nn} = \frac{\begin{vmatrix} J_n(kr_c) & J_n(k_c r_c) \\ J_n'(kr_c) & J_n'(k_c r_c)\sqrt{\frac{\varepsilon_{r_c}}{\mu_{r_c}}} \end{vmatrix}}{\begin{vmatrix} -H_n^{(2)}(kr_c) & J_n(k_c r_c) \\ -H_n^{'(2)}(kr_c) & J_n'(k_c r_c)\sqrt{\frac{\varepsilon_{r_c}}{\mu_{r_c}}} \end{vmatrix}} \tag{23}$$

where r_c is the radius of the cylinder, $k_c = k\sqrt{\varepsilon_{r_c}\mu_{r_c}}$, and ε_{r_c} and μ_{r_c} are, respectively, the relative permittivity and permeability of the cylinder.

Assuming that $d_{nn} = 0$, $\forall n, |n| > N_{sc}$, we can merge (2) and (3) and obtain the total field ($\vec{E} = \vec{E^{in}} + \vec{E^{sc}}$) inside the circular boundary

$$\vec{E} = \sum_{n=-N_i}^{N_i} (J_n(k\rho) + d_{nn} \cdot H_n^{(2)}(k\rho)) i_n e^{jn\phi}\hat{z} \tag{24}$$

And using Maxwell's curl equation, we can also obtain the total magnetic field in the inner region

$$\begin{aligned} &\vec{H} = -\tfrac{1}{jw\mu}\nabla \times \vec{E} = \\ &= -\tfrac{1}{\eta}\sum_{n=-N_i}^{N_i} [\tfrac{n}{k\rho}(J_n(k\rho) + d_{nn}H_n^{(2)}(k\rho))\hat{\rho} + \\ &j(J_n'(k\rho) + d_{nn}H_n^{(2)'}(k\rho))\,\hat{\phi}\Big]\, i_n e^{jn\phi} \end{aligned} \tag{25}$$

In the circular boundary, where the continuity of the fields must be enforced, $\rho = R$, the Bessel functions are constant, and thus the fields of the inner region are reduced to

$$\vec{E} = \sum_{n=-N_i}^{N_i} A_n e^{jn\phi} i_n \hat{z} \tag{26}$$

$$\vec{H} = \sum_{n=-N_i}^{N_i} (B_n\hat{\rho} + C_n\hat{\phi}) e^{jn\phi} i_n \tag{27}$$

where

$$A_n = [J_n(kR) + d_{nn}H_n^{(2)}(kR)] \tag{28}$$

$$B_n = -\frac{1}{\eta}\frac{n}{kR}A_n \tag{29}$$

$$C_n = -\frac{1}{\eta}(J_n'(kR) + d_{nn}H_n^{(2)'}(kR)) \tag{30}$$

Enforcing the continuity of tangential fields on the circular boundary between regions A and B gives

$$\sum_{n=-N_i}^{N_i} A_n e^{jn\phi} i_n = \sum_{n=1}^{M} (a_n e_n^+(\phi) + b_n e_n^-(\phi)) g_n(\phi) \tag{31}$$

$$\begin{aligned} &\sum_{n=-N_i}^{N_i} (B_n(\hat{\rho}.\hat{y}) + C_n(\hat{\phi}.\hat{y})) e^{jn\phi} i_n = \\ &= \sum_{n=1}^{M} (a_n e_n^+(\phi) - b_n e_n^-(\phi)) Y_{0n} g_n(\phi) \end{aligned} \tag{32}$$

where $(\hat{\rho}.\hat{y}) = \sin(\phi)$ and $(\hat{\phi}.\hat{y}) = \cos(\phi)$. In order to obtain a matrix system (31) and (32) must be projected over the modes of either region A or B. Projecting over the inner modes of region B $e^{-jm\phi}$ in both sides of the equality, we obtain

$$\sum_{n=-N_i}^{N_i} I_{mn} i_n = \sum_{n=1}^{M} (J_{mn}a_n + K_{mn}b_n) \tag{33}$$

$$\sum_{n=-N_i}^{N_i} L_{mn} i_n = \sum_{n=1}^{M} (M_{mn}a_n - N_{mn}b_n) \tag{34}$$

where $m \in [-N_i, N_i]$ and

$$I_{mn} = \int_0^{2\pi} A_n e^{jn\cdot\phi} e^{-jm\phi} d\phi \tag{35}$$

$$L_{mn} = \int_0^{2\pi} (B_n \sin(\phi) + C_n \cos(\phi)) e^{jn\phi} e^{-jm\phi} d\phi \tag{36}$$

$$J_{mn} = \int_0^{2\pi} e_n^+(\phi) g_n(\phi) e^{-jm\phi} d\phi \tag{37}$$

$$K_{mn} = \int_0^{2\pi} e_n^-(\phi) g_n(\phi) e^{-jm\phi} d\phi \tag{38}$$

$$M_{mn} = \int_0^{2\pi} e_n^+(\phi) Y_{0n} g_n(\phi) e^{-jm\phi} d\phi = Y_{0n} J_{mn} \tag{39}$$

$$N_{mn} = \int_0^{2\pi} e_n^-(\phi) Y_{0n} g_n(\phi) e^{-jm\phi} d\phi = Y_{0n} K_{mn} \tag{40}$$

Projecting (31) and (32) to the modes of the outer region A $g_m^*(\phi)$ gives

$$\sum_{n=-N_i}^{N_i} O_{mn} i_n = \sum_{n=1}^{M} (P_{mn}a_n + Q_{mn}b_n) \tag{41}$$

$$\sum_{n=-N_i}^{N_i} V_{mn} i_n = \sum_{n=1}^{M} (U_{mn} a_n - T_{mn} b_n) \tag{42}$$

With $m \in [1, M]$ and

$$O_{mn} = \int_0^{2\pi} A_n e^{jn\cdot\phi} g_m^*(\phi) d\phi \tag{43}$$

$$V_{mn} = \int_0^{2\pi} (B_n \sin(\phi) + C_n \cos(\phi)) e^{jn\phi} g_m^*(\phi) d\phi \tag{44}$$

$$P_{mn} = \int_0^{2\pi} e_n^+(\phi) g_n(\phi) g_m^*(\phi) d\phi \tag{45}$$

$$Q_{mn} = \int_0^{2\pi} e_n^-(\phi) g_n(\phi) g_m^*(\phi) d\phi \tag{46}$$

$$U_{mn} = \int_0^{2\pi} e_n^+(\phi) g_n(\phi) Y_{0n} g_m^*(\phi) d\phi = Y_{0n} \cdot P_{mn} \tag{47}$$

$$T_{mn} = \int_0^{2\pi} e_n^-(\phi) g_n(\phi) Y_{0n} g_m^*(\phi) d\phi = Y_{0n} \cdot Q_{mn} \tag{48}$$

Expressing (33), (34), (41) and (42) in matrix form,

$$Ii = Ja + Kb \tag{49}$$

$$Li = Ma - Nb \tag{50}$$

$$Oi = Pa + Qb \tag{51}$$

$$Vi = Ua - Tb \tag{52}$$

In order to obtain the generalized scattering matrix only two equations of the four are required. One equation must be of electric field and another of magnetic field. The only possibility is to use (49) or (50) to extract i, since O and V are not square. If we choose (50) the matrix L must be inverted, but this matrix is bidiagonal and is ill-conditioned. Then (49) must be used for extracting i,

$$i = I^{-1}(Ja + Kb) \tag{53}$$

Now a magnetic field equation must be used. It can be (50) or (52). If we use (52), which comes from enforcing continuity of magnetic field and projecting over modes of region A, we use both the electric and magnetic field and we use one equation with projection over the modes of region A and another equation with projection over the modes of region B. Substituting (53) in (52) and reordering, we obtain the generalized scattering matrix ($b = S\,a$),

$$S = (T + VI^{-1}K)^{-1}(U - VI^{-1}J) \tag{54}$$

The integrals needed to fill matrices I, J, K, V, T and U can be solved either analytically or by using the fast Fourier transform.

B. Solution of the integrals

There are six integrals that need to be solved: I_{mn}, J_{mn}, K_{mn}, V_{mn}, T_{mn} and U_{mn}.

I_{mn} can be solved analytically,

$$I_{mn} = \begin{cases} A_n 2\pi & m = n \\ 0 & m \neq n \end{cases} \tag{55}$$

Since I_{mn} is a diagonal matrix, its inverse is very simple to calculate, just by inverting each element of the main diagonal.

The second integral J_{mn} is

$$J_{mn} = x^{(n)}[-m]\, 2\pi \tag{56}$$

where

$$x^{(n)}[m] = DTFT^{-1}\left\{e_n^+(\phi) g_n(\phi)\right\} \tag{57}$$

In order to obtain $x^{(n)}[m]$ the continuous value of $e_n^+(\phi) g_n(\phi)$ should be considered. We can accelerate the calculus if we consider the value of $e_n^+(\phi) g_n(\phi)$ only over some discrete points along ϕ, using the fast Fourier transform,

$$x^{(n)}[m] \approx \tilde{x}^{(n)}[m] = FFT^{-1}\left\{e_n^+(\phi) g_n(\phi)\right\} \tag{58}$$

$\tilde{x}^{(n)}$ is a periodic signal of period equal to the number of discrete points considered along ϕ for performing the fast Fourier transform. Nevertheless the duration of the original signal $x^{(n)}[m]$ can exceed that period, and therefore an error of aliasing can appear. In order to minimize this error we must choose a proper number of points for the fast Fourier transform. This number of points must be at least of $2N_i + 1$ (the number of rows of J), and we will use $Nfft \geq 2N_i + 1$ points. As $Nfft$ increases, the error due to aliasing decreases.

Using the fast Fourier transform the remaining integrals can also be easily obtained,

$$K_{mn} = \approx 2\pi\, \tilde{x}^{-(n)}[-m] \tag{59}$$

$$V_{mn} = \approx \pi \tilde{y}^{(m)}[n+1]\,[C_n - jB_n] + \tag{60}$$

$$+\pi \tilde{y}^{(m)}[n-1]\,[C_n + jB_n] \tag{61}$$

$$T_{mn} = \approx Y_{0n} \sum_{k=-\frac{Nfft}{2}}^{\frac{Nfft}{2}} \tilde{x}^{-(n)}[k]\, \tilde{y}^{(m)}[-k]\, 2\pi \tag{62}$$

$$U_{mn} = \approx Y_{0n} \sum_{k=-\frac{Nfft}{2}}^{\frac{Nfft}{2}} \tilde{x}^{(n)}[k]\, \tilde{y}^{(m)}[-k]\, 2\pi \tag{63}$$

where

$$\tilde{x}^{-(n)}[m] = FFT^{-1}\left\{e_n^-(\phi) g_n(\phi)\right\} \tag{64}$$

$$\tilde{y}^{(m)}[n] = FFT^{-1}\left\{g_m^*(\phi)\right\} \tag{65}$$

C. Study of the parameters that control the method

For computational reasons there are several summations with infinite terms that must be truncated in order to obtain the scattering parameters of the structure. For that purpose the following truncation indexes have been defined:

- Number of modes of the incident field spectrum: $N_i = P_{N_i}\, k\, R$
- Number of points for the FFT: $N_{fft} = 2\text{ceil}(N_i(1 + P_{N_{fft}})) + 1$

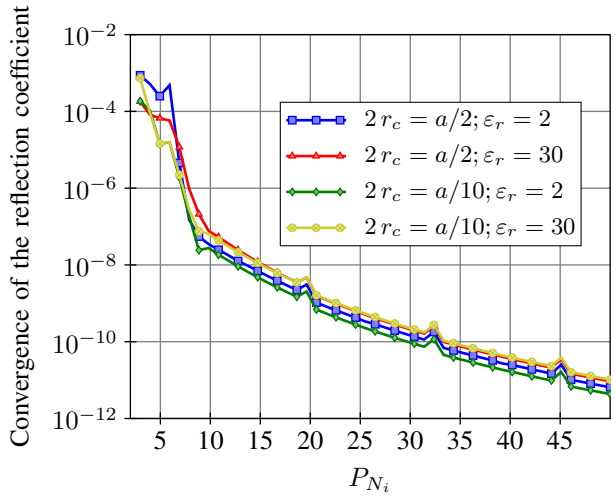

Fig. 3. Convergence of the reflection coefficient with P_{N_i}

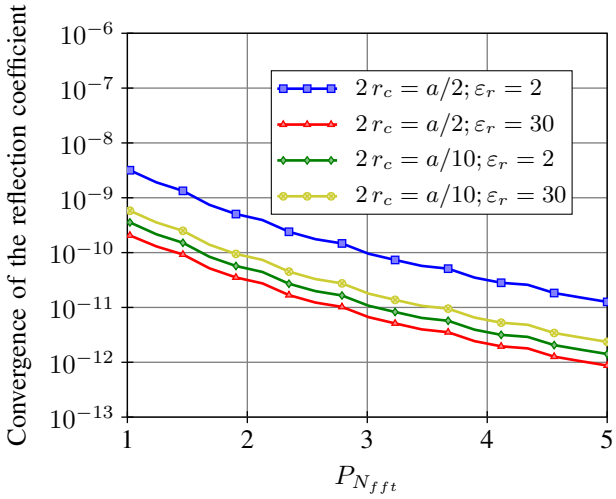

Fig. 4. Convergence of the reflection coefficient with $P_{N_{fft}}$

The number of modes for the scattered field spectrum N_{sc} has been fixed to $2k\,r_a$, since according to [29] it is enough to consider $N_{sc} \geq k\,r_a$.

In order to test the convergence of the method and choose the adequate values for these indexes the convergence (difference with the previous value) of the computed S_{11} scattering parameter with each one of these indexes has been represented. In all the graphics there are four plots representing four different combinations of post size and electric permittivity: large and small posts with either high or small permittivity. This ensures that the chosen value for the truncation indexes are valid for a wide range of post types.

Fig. 3 shows the convergence of S_{11} with the parameter (P_{N_i}) that controls the number of modes of the incident field spectrum (N_i). The value of P_{N_i} is gradually increased and the variation of S_{11} with the previous value of P_{N_i} is depicted. As the number of modes of the incident field spectrum increases, the value of S_{11} is stabilized, and the difference with the previous value is constantly decreased. This convergence in the value of S_{11} does not depend on the size or permittivity of the post. The value P_{N_i}=15 has been chosen for all calculations because the value of S_{11} is already stabilized to variations under -160 dB, which ensures a very good accuracy. Greater values of P_{N_i} would not significantly increase the accuracy at the cost of highly increasing the computational cost.

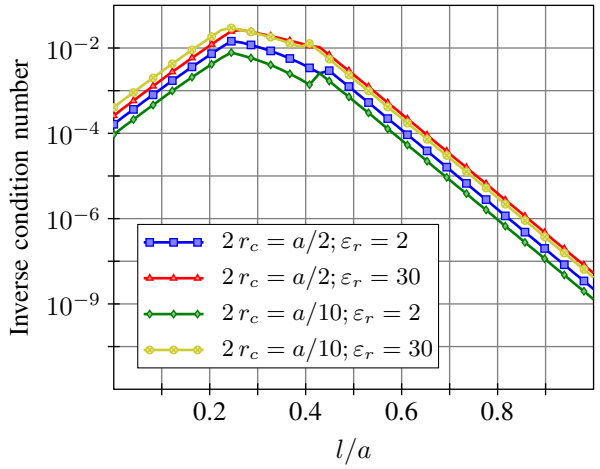

Fig. 5. Inverse condition number as a function of the distance to the reference planes

Fig. 4 shows the convergence of S_{11} with $P_{N_{fft}}$. Again the convergence does not depend on the post size and permittivity. $P_{N_{fft}}$=2 is the value chosen to ensure very good accuracy and low computational cost.

The circular boundary chosen for the mode matching simplifies the expressions of the cylindrical modes in that surface, but this implies that the propagation exponentials of the guided waves are not constant as happens when the transversal section of the guide is chosen as boundary for the mode matching. For that reason there is certain sensitivity of the method to the placement of the reference planes. Fig. 5 shows the dependence of the reciprocal of the condition number of the matrix that is inverted in (54) in the 1-norm with the distance from the reference planes of the input and output waveguides to the center of the dielectric cylinder (l). It can be observed that there is an optimum distance $l = 0,25\,a$ for the reference planes where the matrix is better conditioned.

IV. Arbitrarily Shaped Obstacles

A. General theory

The method can be extended to other problems than the single centered circular post. The most important difference is that the scattering matrix D that relates incident and scattered field spectra will not be a diagonal matrix any more, even for a circular post if it is not placed at the center of the waveguide.

As in the case of the centered circular post the generalized scattering matrix can be obtained using (54), and the matrices involved in that equation are the ones described in section III-B except for matrices I and V that change due to the change of matrix D which is no longer diagonal.

Matrix I comes from projecting the transversal electric field of the inner region on the circular boundary to the cylindrical modes, which using (2) and (5) gives,

$$\begin{aligned} I_{mn} &= \int_0^{2\pi} E_t(\rho=R)\cdot e^{-jm\phi} \\ &= \sum_{n=-N_i}^{N_i} \left(J_n(kR)\int_{2\pi}^{0} e^{j(n-m)\phi}d\phi + \right. \\ &\left. \sum_{q=-N_{sc}}^{N_{sc}} d_{qn}H_q^{(2)}(kR)\int_{2\pi}^{0} e^{j(q-m)\phi}d\phi\right) \end{aligned} \quad (66)$$

Defining

$$\begin{aligned} I^A_{mn} &= J_n(kR)\int_0^{2\pi} e^{j(n-m)\phi}d\phi \\ &= \begin{cases} J_n(kR)2\pi & n=m \\ 0 & n\neq m \end{cases} \end{aligned} \quad (67)$$

$$\begin{aligned} I^B_{mn} &= H_q^{(2)}(kR)\int_0^{2\pi} e^{j(q-m)\phi}d\phi \\ &= \begin{cases} H_n^{(2)}(kR)2\pi & n=m \\ 0 & n\neq m \end{cases} \end{aligned} \quad (68)$$

the new matrix I can be written as

$$I = I^A + I^B D \quad (69)$$

Matrix V comes from projecting the transversal magnetic field of the inner region on the circular boundary to the guided modes. The transversal magnetic field of the inner region on the circular boundary is

$$\begin{aligned} &H_t(\rho=R) = \\ &\sum_{n=-N_i}^{N_i}\left[-\frac{\sin\phi}{\eta\, kR}\left(nJ_n(kR)e^{jn\phi}+\sum_q qd_{qn}H_q^{(2)}(kR)e^{jq\phi}\right)\right. \\ &\left.-\frac{j\cos\phi}{\eta}\left(J_n'(kR)e^{jn\phi}+\sum_q d_{qn}H_q^{(2)'}(kR)e^{jq\phi}\right)\right] i_n \end{aligned}$$

Projecting to guided modes

$$V_{mn} = \int_0^{2\pi} H_t(\rho=R)\, g_m^*(\phi)d\phi$$

$$\begin{aligned} &V_{mn} = \textstyle\int_0^{2\pi} -\frac{1}{\eta}\frac{n}{kR}J_n(kR)e^{jn\phi}(\frac{e^{j\phi}-e^{-j\phi}}{2j})g_m^*(\phi)d\phi + \\ &+\textstyle\int_0^{2\pi} -\frac{1}{\eta}\frac{q}{kR}\sum_q d_{qn}H_q^{(2)}(kR)e^{jq\phi}(\frac{e^{j\phi}-e^{-j\phi}}{2j})g_m^*(\phi)d\phi + \\ &+\textstyle\int_0^{2\pi} -\frac{j}{\eta}J_n'(kR)e^{jn\phi}(\frac{e^{j\phi}+e^{-j\phi}}{2})g_m^*(\phi)d\phi + \\ &+\textstyle\int_0^{2\pi} -\frac{j}{\eta}\sum_q d_{qn}H_q^{(2)'}(kR)e^{jq\phi}(\frac{e^{j\phi}+e^{-j\phi}}{2})g_m^*(\phi)d\phi \end{aligned} \quad (70)$$

Using (65) and the properties of the discrete time Fourier transform,

$$\frac{1}{2\pi}\int_0^{2\pi} g_m^*(\phi)e^{j\phi}e^{jn\phi}d\phi = y^{(m)}[n+1] \simeq \tilde{y}^{(m)}[n+1] \quad (71)$$

$$\frac{1}{2\pi}\int_0^{2\pi} g_m^*(\phi)e^{-j\phi}e^{jn\phi}d\phi = y^{(m)}[n-1] \simeq \tilde{y}^{(m)}[n-1] \quad (72)$$

Substituting in (70),

$$\begin{aligned} &V_{mn} \simeq -\tfrac{\pi}{\eta}\tfrac{n}{kR}\tfrac{J_n(kR)}{j}(\tilde{y}^{(m)}[n+1]-\tilde{y}^{(m)}[n-1])+ \\ &-\tfrac{\pi}{\eta}\tfrac{q}{kR}\textstyle\sum_q d_{qn}\tfrac{H_q^{(2)}(kR)}{j}(\tilde{y}^{(m)}[q+1]-\tilde{y}^{(m)}[q-1])+ \\ &-\tfrac{j\pi}{\eta}J_n'(kR)(\tilde{y}^{(m)}[n+1]+\tilde{y}^{(m)}[n-1])+ \\ &-\tfrac{j\pi}{\eta}\textstyle\sum_q d_{qn}H_q^{(2)'}(kR)(\tilde{y}^{(m)}[q+1]+\tilde{y}^{(m)}[q-1]) \end{aligned} \quad (73)$$

In matrix form,

$$V = \pi Y^+(V^A + V^B D) + \pi Y^-(V^C + V^D D) \quad (74)$$

Where

$$Y^+ = \begin{bmatrix} \tilde{y}^{(1)}[n+1] \\ \tilde{y}^{(2)}[n+1] \\ . \\ . \\ \tilde{y}^{(M)}[n+1] \end{bmatrix}_{M\times(2N_i+1)} \quad (75)$$

$$Y^- = \begin{bmatrix} \tilde{y}^{(1)}[n-1] \\ \tilde{y}^{(2)}[n-1] \\ . \\ . \\ \tilde{y}^{(M)}[n-1] \end{bmatrix}_{M\times(2N_i+1)} \quad (76)$$

and V^A, V^B, V^C and V^D are diagonal matrices with

$$V^A_{nn} = -\frac{1}{\eta}\frac{n}{kR}\frac{J_n(kR)}{j} - \frac{jJ_n'(kR)}{\eta} \quad (77)$$

$$V^B_{nn} = \frac{1}{\eta}\frac{n}{kR}\frac{J_n(kR)}{j} - \frac{jJ_n'(kR)}{\eta} \quad (78)$$

$$V^C_{nn} = -\frac{1}{\eta}\frac{n}{kR}\frac{H_q^{(2)}(kR)}{j} - \frac{jH_q^{(2)'}(kR)}{\eta} \quad (79)$$

$$V^D_{nn} = \frac{1}{\eta}\frac{n}{kR}\frac{H_q^{(2)}(kR)}{j} - \frac{jH_q^{(2)'}(kR)}{\eta} \quad (80)$$

Using (54) and the expressions of section III-B substituting I and V with (69) and (74) we obtain the generalized scattering matrix of any arbitrarily shaped single or multiple obstacle geometry inside a rectangular waveguide. For each specific obstacle the problem is now reduced to the computation of the open space scattering matrix D.

If the post is circular matrix D can be found analytically, as shown in (22) and (23). For other geometries, i. e. a square post, the scattering matrix must be obtained using a suitable numerical method such as the method of moments.

If there is a single off-centered post, the matrix D can be obtained as

$$D = TJ^{BA}D_cTJ^{AB} \quad (81)$$

where D_c is the scattering matrix of the centered circular post and TJ^{BA} and TJ^{AB} are translation matrices that translate cylindrical field spectrum either from A to B or from B to A using the addition theorem for Bessel functions (see [29], [31], [32]).

If there are multiple scattering posts inside region B (see Fig. 1), the method described in [33] can be used to analytically obtain the joint scattering matrix D once the individual scattering matrices of each scatterer have been computed.

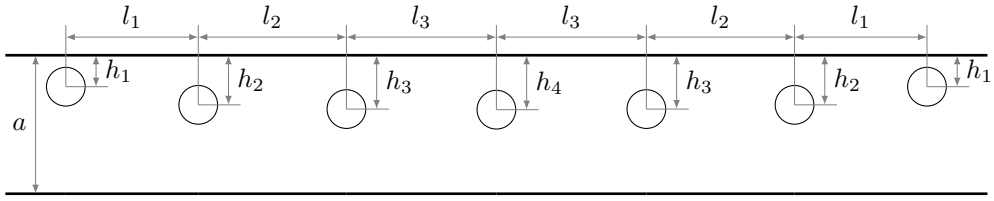

Fig. 10. Geometry of a constant diameter off-centered single metallic rod filter

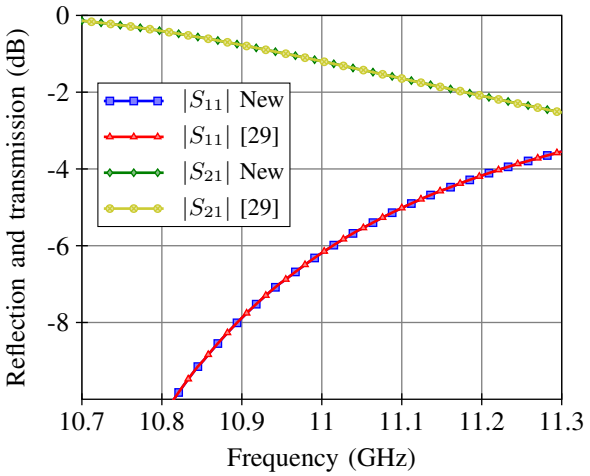

Fig. 6. Single centered dielectric post. $a = 19.05$ mm, $r_c = 0.11\,a$, $\varepsilon_{r_c} = 24$.

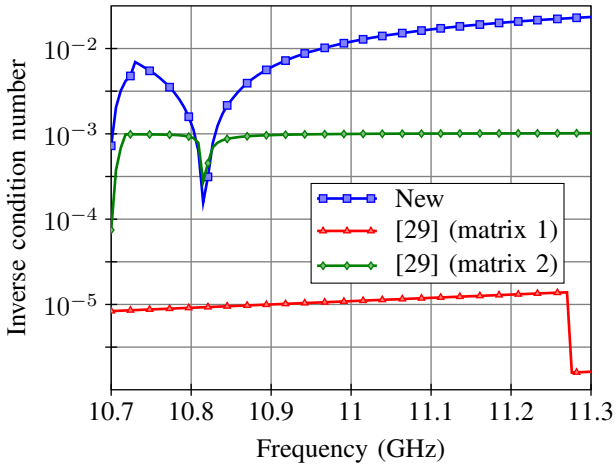

Fig. 7. Inverse condition number as a function of the frequency for a centered dielectric post. $a = 19.05$ mm, $r_c = 0.11\,a$, $\varepsilon_{r_c} = 24$.

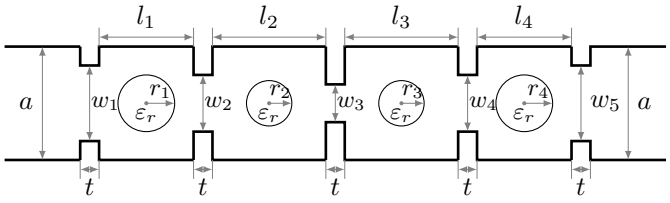

Fig. 8. Four pole H-plane cavities filter loaded with centered cylindrical resonators. a=19,05 mm, ε_r=24, $l_1 = l_4$=6,98 mm, $l_2 = l_3$=8,28 mm, $w_1 = w_5$=13,37 mm, $w_2 = w_4$=6,286 mm, w_3=6,1 mm, t=2 mm, $r_1 = r_4$=2,111 mm, $r_2 = r_3$=2,172 mm.

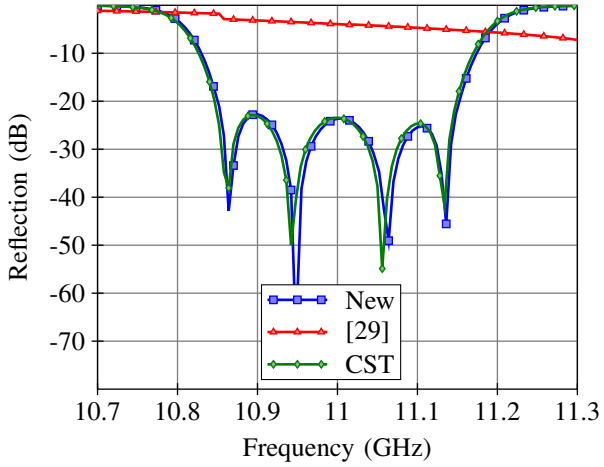

Fig. 9. Reflection coefficient of the cavities filter loaded with dielectric cylinders

V. Results

The new method presented in this paper has been first tested with the analysis of a single centered circular post. Results are shown in Fig. 6 and compared with the results provided by the method presented in [29] by Esteban *et al.* Although there is a good agreement between both results, the new method is much more accurate. In [29] two matrices had to be inverted in order to obtain the scattering parameters, whereas the new method only needs to invert one matrix (see (54)). Furthermore, the matrix in (54) is better conditioned than the matrices in [29], as shown in Fig. 7. Although this circumstance does not imply a significant difference between both methods for the results of the fundamental mode, as shown in Fig. 6, the method of [29] has very poor accuracy for high order modes, and when the generalized scattering matrix of the post is cascaded with the multimodal matrices of adjacent building blocks (steps, lines) of the structure the overall accuracy rapidly decreases, and the results provided for the whole filter response has a very poor convergence.

In [36] and [37] the method of [29] was used to analyze a four pole coupled cavities filter loaded with centered circular cylinders (see geometry in Fig. 8). The results were accurate only for 11 guided modes. If a lower or higher number of guided modes was used, the results became inaccurate. This poor convergence of the method of [29] can be appreciated in Fig. 9, where the results are computed with the method of [29] using 15 guided modes, and the results have completely diverged. This poor converge proved to be due to the bad

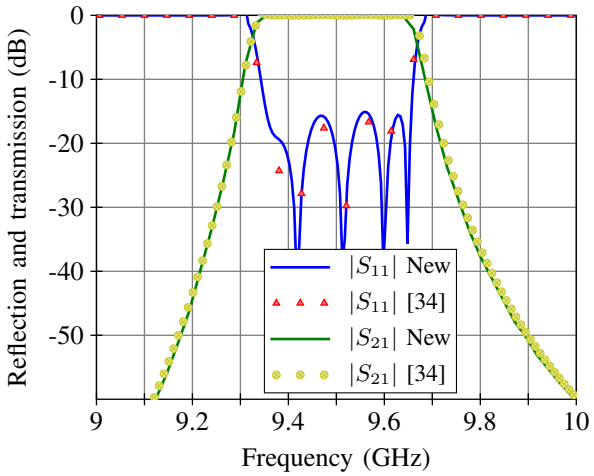

Fig. 11. Scattering parameters of a constant diameter off-centered single metallic rod filter. a=22.86 mm, rod radii=3.21 mm, h_1=5.215 mm, h_2=8.172 mm, h_3=8.863 mm, h_4=8.971 mm, l_1=21.895 mm, l_2=24.461 mm, l_3=24.797 mm.

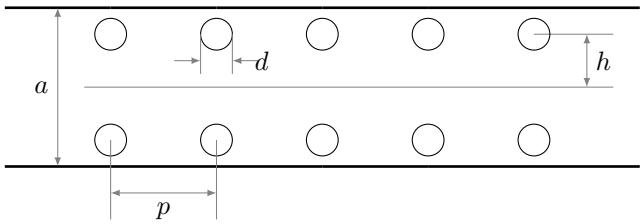

Fig. 12. Geometry of a rectangular waveguide filter periodically loaded with double cylindrical posts

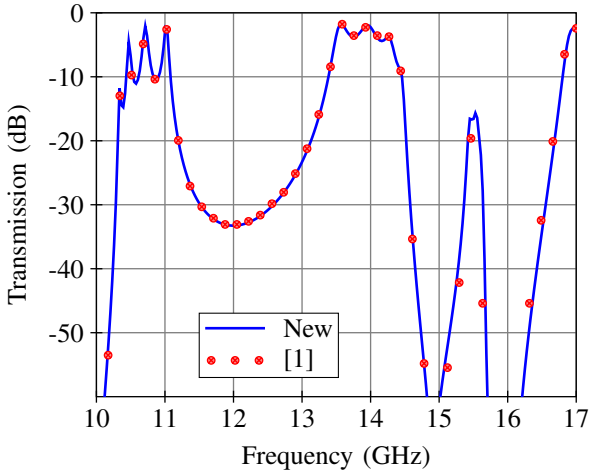

Fig. 13. Scattering parameters of a rectangular waveguide periodically loaded with double cylindrical posts. a=22.86 mm, p=15.7 mm, h=7.8 mm,d=4 mm, $\varepsilon_r = 14.8\,(1 - j0,005)$.

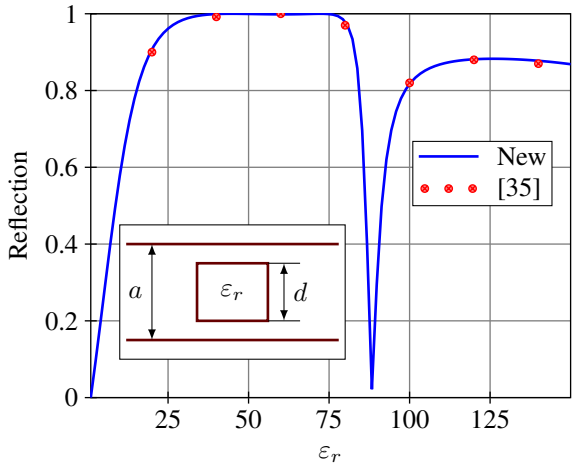

Fig. 14. Reflection of a square dielectric post centered in a rectangular waveguide as a function of the relative electric permittivity ε_r (d/a=0.1, $\lambda/1$=1.4)

conditioning of the matrix that had to be inverted when the reference planes had to be placed close to the center of the post, and this fact lead us to develop a new method that could overcome this limitation. Fig. 9 shows that the new method, presented in this paper, provides very accurate results, in good agreement with the results from the CST commercial software. This results are stable with the number of guided modes once the convergence has been reached at approximatedly 7 guided modes. The CPU time required with a PIV processor at 2.4 GHz was 24 seconds per frequency point with CST and 0.05 seconds with the method of [29], whereas the new method only required 0.03 seconds. The generalized scattering matrices of the empty lines have been obtained analytically using standard transmission line theory, and the generalized scattering matrices of the steps have been computed using the well-known mode matching method [8].

The new method has also been tested with the analysis of an H-plane filter loaded with constant diameter off-centered circular metallic cylinders (see Fig. 10 and 11), and with an H-plane filter periodically loaded with double cylindrical lossy dielectric posts (see Fig. 12 and 13). In both cases the results provided with the new method are in good agreement with the results from the literature. The CPU time required was, respectively, 0.04 and 0.05 seconds per frequency point.

The new method can also be used for the analysis of arbitrarily shaped, non-circular rods. Figure 14 shows the analysis of a square dielectric post inside a rectangular waveguide. Since the post is not circular, the numerical method of [38] has been used to compute the open space scattering matrix D. This reduces the efficiency, and while the analysis of the circular post inside the waveguide needs only 0.005 seconds, the square post needs 0.035 seconds.

VI. Conclusions

A new hybrid open space and guided modes mode matching method for the analysis of H-plane single or multiple obstacles inside a rectangular waveguide has been presented. The use of a circular boundary to match guided and open space cylindrical

modes avoids the walls of the guide and allows the solution of the required integrals using the fast Fourier transform algorithm. The efficiency of this technique is maximum for circular obstacles, though the method is valid for general arbitrarily shaped posts. The new mode matching procedure overcomes the limitation of a previous method that provided accurate results only for the fundamental mode. The new method is better conditioned, highly accurate also for high order modes, and reduces the computation time by approximately 40%. The new method has been tested with the analysis of a single circular post and several filter topologies with single and multiple circular posts.

VII. Acknowledgment

This work has been supported by Ministerio de Ciencia e Innovación, Spanish Government, under the framework of coordinated research project TEC 2007-67630-C03-01.

References

[1] R. Lech and J. Mazur, "Propagation in rectangular waveguides periodically loaded with cylindrical posts," *IEEE Microwave and Wireless Components Lett.*, vol. 14, no. 4, pp. 177–179, April 2004.

[2] J. K. Plourde and C. Ren, "Applications of dielectric resonators in microwave components," *IEEE Trans. Microwave Theory Tech.*, vol. 29, pp. 754–770, August 1981.

[3] C.-I. Hsu and A. Auda, "Multiple dielectric posts in a rectangular waveguide," *IEEE Trans. Microwave Theory Tech.*, vol. 34, no. 8, pp. 883–891, August 1986.

[4] P. Arcioni, V. E. Boria, M. Bozzi, G. Conciauro, and B. Gimeno, "Analysis of H-plane waveguide components with dielectric obstacles by the BI-RME method," in *Proc. of the 32nd Eu. Microwave Conf.*, Milano, 2002, pp. 1–3.

[5] C. Bachiller, H. Esteban, F. Diaz, V. Boria, and J. Morro, "Comparative study of multipactor breakdown in waveguide H-plane filters loaded with dielectric resonators," in *Int. Workshop on Multipactor, Corona and Passive Intermodulation*, Valencia, Sept. 2008, pp. 1–8.

[6] C. Bachiller, H. Esteban, V. E. Boria, A. Belenguer, and J. V. Morro, "Efficient technique for the cascade connection of multiple two port scattering matrices," *IEEE Transactions on Microwave Theory and Techniques*, vol. 55, no. 9, pp. 1880–1886, September 2007.

[7] D. M. Pozar, *Microwave Engineering*. USA: Wiley & Sons, 2005.

[8] J. Reiter and F. Arndt, "Rigorous analysis of arbitrarily shaped H- and E-plane discontinuities in rectangular waveguides by a full-wave boundary contour mode-matching method," *IEEE Trans. Microwave Theory Tech.*, vol. 43, no. 4, pp. 796–801, April 1995.

[9] G. Gerini, M. Guglielmi, and G. Lastoria, "Efficient integral equation formulations for admittance or impedance representation of planar waveguide junctions," *IEEE MTT-Symp. Dig.*, vol. III, pp. 1747–1750, 1998.

[10] N. Marcuwitz, *Waveguide Handbook*. New York: McGraw-Hill, 1951.

[11] L. Lewin, *Advanced Theory of Waveguides*. London: McGraw-Hill, 1951.

[12] J. C. Araneta, M. E. Brodwin, and G. A. Kriegsmann, "High-temperature microwave characterization of dielectric rods," *IEEE Trans. Microwave Theory Tech.*, vol. 32, no. 10, pp. 1328–1334, October 1984.

[13] Y. Leviatan., P. Li, A. Adams, and J. Perini, "Single-post inductive obstacle in rectangular waveguide," *IEEE Trans. Microwave Theory Tech.*, vol. 31, no. 10, pp. 806–811, Oct. 1983.

[14] Y. Leviatan., D. Shau, and A. T. Adams, "Numerical study of the current distribution on a post in a rectangular waveguide," *IEEE Trans. Microwave Theory Tech.*, vol. 32, pp. 1411–1415, Oct. 1984.

[15] Y. Leviatan and G. Sheaffer, "Analysis of inductive dielectric posts in rectangular waveguide," *IEEE Trans. Microwave Theory Tech.*, vol. 35, no. 1, pp. 48–59, Jan. 1987.

[16] G. Sheaffer and Y. Leviatan, "Composite inductive posts in waveguide - a multifilament analysis," *IEEE Trans. Microwave Theory Tech.*, vol. 36, no. 4, pp. 779–783, April 1988.

[17] M. Koshiba and M. Suzuki, "Finite-element analysis of H-plane waveguide junction with arbitrarily shaped ferrite post," *IEEE Trans. Microwave Theory Tech.*, vol. 34, no. 1, pp. 103–109, Jan. 1986.

[18] K. Ise and M. Koshiba, "Equivalent circuits for dielectric posts in a rectangular waveguide," *IEEE Trans. Microwave Theory Tech.*, vol. 37, no. 11, pp. 1823–1825, Nov. 1989.

[19] ——, "Dielectric post resonances in a rectangular waveguide," *IEE Proceedings*, vol. 137, no. 1, pp. 61–66, February 1990.

[20] H. A. Auda and C. E. Smith, "The rsonances method for evaluating the impedances of the equivalent network for dielectric posts in a rectangular waveguide," *IEEE Trans. Microwave Theory Tech.*, vol. 38, no. 11, pp. 1595–1601, November 1990.

[21] V. Catina, F. Arndt, and J. Brandt, "A surface integral equation formulation for dielectric post structures in waveguides," *IEEE MTT-S International Microwave Symposium*, pp. 1–4, November 2005.

[22] M. Bhattacharya and B. Gupta, "Neural network model of s-parameters for a dielectric post in rectangular waveguide," in *Proc. of the Int. Conf. on Recent Advances in Microwave Theory and Applications*, Atlanta, 21-24 Nov. 2008, pp. 581–583.

[23] E. D. Nielsen, "Scattering by a cylindrical post of complex permittivity in a waveguide," *IEEE Trans. Microwave Theory Tech.*, vol. MTT-17, no. 3, pp. 148–153, 1969.

[24] L. Lewin, "On the inadequacy of discrete mode-matching techniques in some waveguide discontinuity problems," *IEEE Trans. Microwave Theory Tech.*, vol. 18, pp. 364–372, 1970.

[25] J. N. Sahalos and E. Vafiadis, "On the narrow-band microwave filter design using a dielectric rod," *IEEE Trans. Microwave Theory Tech.*, vol. 33, no. 11, pp. 1165–1171, November 1985.

[26] R. Geshe and N. Lochel, "Scattering by a lossy dielectric cylinder in a rectangular waveguide," *IEEE Trans. Microwave Theory Tech.*, vol. 36, no. 1, pp. 137–144, Jan. 1988.

[27] ——, "Two cylindrical obstacles in a rectangular waveguide – resonances and filter applications," *IEEE Trans. Microwave Theory Tech.*, vol. 37, no. 6, pp. 962–968, June 1989.

[28] J. Abdulnour and L. Marchildon, "Scattering by a dielectric obstacle in a rectangular waveguide," *IEEE Trans. Microwave Theory Tech.*, vol. 41, no. 11, pp. 1988–1994, November 1993.

[29] H. Esteban, S. Cogollos, V. E. Boria, A. S. Blas, and M. Ferrando, "A new hybrid mode-matching/numerical method for the analysis of arbitrarily shaped inductive obstacles and discontinuities in rectangular waveguides," *IEEE Trans. Microwave Theory Tech.*, vol. 50, no. 4, pp. 1219–1224, April 2002.

[30] C. Balanis, *Advanced Engineering Electromagnetics*. John Wiley & Sons, 1989.

[31] A. Elsherbeni, M. Hamid, and G. Tian, "Iterative scattering of a gaussian beam by an array of circular conducting and dielectric cylinders," *J. of Electromagnetic Waves and Applications*, vol. 7, no. 10, pp. 1323–1342, 1993.

[32] R. Harrington, *Time-Harmonic Electromagnetic Fields*. New York: McGraw-Hill Book Company, 1961.

[33] H. Esteban, S. Cogollos, C. Bachiller, A. S. Blas, and V. E. Boria, "A new analytical method for the analysis of multiple scattering problems using spectral techniques," in *IEEE Antennas and Propagat. Society Int. Symp.*, San Antonio Texas, Junio 2002, pp. 82–85.

[34] S. Yin, T. Vasilyeva, and P. Pramanick, "Use of three-dimensional field simulators in the synthesis of waveguide round rod bandpass filters," *Int J RF and Microwave CAE*, vol. 8, pp. 484–487, 1998.

[35] J. Abdulnour and L. Marchildon, "Boundary elements and analytic expansions applied to H-plane waveguide junctions," *IEEE Trans. Microwave Theory Tech.*, vol. 42, no. 6, pp. 1038–1045, June 1994.

[36] C. Bachiller, H. Esteban, V. E. Boria, J. V. Morro, L. J. Roglá, M. Taroncher, and A. Belenguer, "Efficient CAD tool for direct-coupled-cavities filters with dielectric resonators," in *2005 IEEE AP-S Int. Symp. Dig.*, vol. 1B, Washington D.C., June 2005, pp. 578–581.

[37] J. V. Morro, C. Bachiller, H. Esteban, and V. E. Boria, "New efficient and robust automated design strategy for H plane direct-coupled-cavities filters with dielectric resonators," in *Proc. of the 2006 AP-S Int. Symp., pp. 597-600*, Alburquerque, June 2006, pp. 597–600.

[38] J. H. Richmond, "Scattering by a dielectric cylinder of arbitrary cross-section shape," *IEEE Trans. Antennas Propagat.*, vol. 13, no. 3, pp. 334–341, May 1965.

Carmen Bachiller (GSM'05) received her degree in Communication Engineering from the Polytechnic University of Valencia in 1996. She worked from 1997 to 2001 in the company ETRA I+D, S.A as a Project Engineer in research and development on automatic traffic control, public transport management and public information systems using telecommunication technology. In 2001 she joined the Communication Department of the Polytechnic University of Valencia as an lecturer. She is teaching signal and systems theory and microwaves. She has participated in several teaching innovation projects. She is now working in her Ph.D. Thesis on electromagnetism and radiofrequency circuits.

Héctor Esteban (S'93-M'99) received the degree in Telecommunications Engineering from the Polytechnic University of Valencia, Spain, in 1996, and the Ph.D. degree in 2002. He collaborated with the Joint Research Center, European Commission, Ispra, Italy. In 1997, he was with the European Topic Center on Soil (European Environment Agency). He rejoined the UPV in 1998. His research interests include methods for the full- wave analysis of open-space and guided multiple scattering problems, CAD design of microwave devices, electromagnetic characterization of dielectric and magnetic bodies, and the acceleration of electromagnetic analysis methods using the wavelets and the FMM.

María Ángeles Valdés received the degree in Telecommunications Engineering from the Polytechnic University of Valencia, Spain, in 2008. She made her final project degree in the study of open space analysis and CAD design of microwave devices and electromagnetic characterization of dielectric bodies. She currently deepens her professional training by attending an official master of biomedical engineer organized jointly by Polytechnic University of Valencia and University of Valencia.

Hilario Mata received the degree in Telecommunications Engineering from the Polytechnic University of Valencia, Spain, in 2006. He received an MBA from ESIC Business & Marketing School in 2006. He had a work experience in Regus Group in London as IT and general assistant in 2007. In 2007 he started to work in INSA as SAP consultant for IBM, working in different projects implementing ERPs for healthcare systems where he keeps working nowadays.

Vicente E. Boria (S'91-A'99-SM'02) received the *Ingeniero de Telecomunicación* and the *Doctor Ingeniero de Telecomunicación* degrees from the Universidad Politécnica de Valencia, Valencia, Spain, in 1993 and 1997, respectively. In 1993 he joined the *Departamento de Comunicaciones*, Universidad Politécnica de Valencia, where he is Full Professor (since 2003). In 1995 and 1996 he was held a Spanish Trainee position with the European Space research and Technology Centre (ESTEC)-European Space Agency (ESA), Noordwijk, the Netherlands. Since 2003, he has served on the Editorial Boards of the IEEE Transactions on Microwave Theory and Techniques. He is also member of the Technical Committees of the IEEE-MTT International Microwave Symposium and of the European Microwave Conference. His current research interests include numerical methods for the analysis of waveguide and scattering structures, automated design of waveguide components, radiating systems, measurement techniques, and power effects in passive waveguide systems.

Ángel Belenguer (M'04) received the Telecommunication Engineering and Ph.D. degrees from the Universidad Politécnica de Valencia, Spain, in 2000 and 2009, respectively. He joined the Universidad de Castilla-La Mancha in 2000, where he is now Profesor Titular de Escuela Universitaria in the Departamento de Ingeniería Eléctrica, Electrónica, Automática y Comunicaciones. His research interests include methods in the frequency domain for the full-wave analysis of open-space and guided multiple scattering problems, specifically the improvement or acceleration of these methods using several strategies: hybridization of two or more different methods, the use of specific basis, and the application of accelerated solvers or solving strategies (like grouping) to new problems or structures.

José Vicente Morro (GSM'02) received the Telecommunications Engineering degree from the Universidad Politécnica de Valencia (UPV), Valencia, Spain, in 2001, and is currently pursuing his Ph.D. degree at UPV. In 2001, he became a Research Fellow with the Departamento de Comunicaciones, UPV. In 2003 he joined the Signal Theory and Communications Division, Universidad Miguel Hernández, where he was a Lecturer. In 2005, he rejoined the Departamento de Comunicaciones, UPV, as an Assistant Lecturer. His current interests include CAD design of microwave devices and EM optimization methods.